Digital Signal Processing Algorithms for the Detection of Afferent Nerve Activity Recorded from Cuff Electrodes

Barry Upshaw and Thomas Sinkjær, *Member, IEEE*

***Abstract*—Due to the very poor signal-to-noise ratios (SNR's) usually encountered with whole nerve-cuff signals, the processing method typically applied, rectification and windowed (bin)-integration (RBI), can have serious shortcomings in extracting reliable information. In order to improve detection accuracy, these signals were further analyzed using statistical signal detection algorithms based on their second and higher order spectra (HOS). A comparison with both analog and digital RBI processing suggests that the statistical methods, due to their ability to separate the signal and noise subspaces, are superior. It was determined that the noise typically encountered with nerve-cuff electrode signals is normally (Gaussian) distributed. Therefore, third-order statistics can be applied to, ideally, completely reject the noise component. When cutaneous nerve recordings from the *calcaneal* nerve (innervating the heel area) were used in a drop-foot correction neural prosthesis, the detection percentage and the insensitivity to algorithm parameters were increased through the use of these statistical methods as to warrant their real-time implementation, and the inherent additional processing hardware that entails.**

***Index Terms*—Drop-foot correction, real-time implementation, statistical signal detection, whole nerve-cuff signals.**

I. Introduction

IT has been demonstrated in human subjects that afferent nerve signals can be used as a replacement for artificial sensors in neural prostheses for both the upper and lower extremities, [1], [2]. In this type of application, where stable, chronic recording is required, the use of nerve-cuff electrodes has proven particularly suitable, [3]. These electrodes, typically made from silicone tubing and stainless-steel wire, allow a measure of the electrical activity in the nerve to be recorded directly as a potential difference, [4]. Unfortunately, due to the low current densities traveling within sensory nerve fibers, these potentials are very low (in the μV range), and therefore subject to interference from sources inside the body (primarily muscle activation potentials), as well as from external sources (mains power, electronic devices, etc.). Thus, although conceptually promising, afferent nerve signals recorded from nerve-cuff electrodes are difficult to use in practice, due to the poor overall signal-to-noise ratios (SNR's) typically seen. The problems in extracting useful information from these signals have been cited as potential obstacles to their application, [5]. It is likely, however, that improvements will be made on three fronts: 1) better nerve/electrode interfaces [6], 2) improved analog processing and amplification circuitry [7], and 3) improved signal processing.

Two advanced signal processing algorithms, both based upon signal and noise subspace orthogonal decompositions using the signal's *statistical* distribution are of particular interest when focusing on improved signal processing. The first algorithm, which is based on a second-order signal statistic (autocorrelation), is quite similar to the well-known *super-resolution* algorithms (MUSIC, for example) for performing an analysis of the signal's principal components, [8]. The second algorithm is based upon a higher order statistic (HOS) of the signal. Both perform an orthogonal decomposition and derive an eigenvalue-spectrum, utilizing a singular value decomposition (SVD), or other diagonalization methods. Both of these algorithms have successfully been used in implementing robust detectors for the presence of speech signals corrupted with high powered background noise, [9]. In this study the performance of these algorithms is compared with that of the most commonly applied "real-time" processing method, namely, integration of the rectified (and filtered) signal, [10]. Typically referred to as rectification and windowed (bin)-integration (RBI) processing, designating the primary steps of rectification and bin-integration [or, alternatively, the integral of the absolute value (IAV)], this method is both simple to implement, and performs reliably in high SNR applications, [11].

Before attempting to design optimal detection algorithms, it is advantageous that the characteristics of both the signal-of-interest (SOI), and the contaminating noise be known. This is especially true if these characteristics prove to be stationary. It is known from previous work with cuff electrodes that the SOI is bandlimited, [1]. Unfortunately, little information about the statistical properties of either the signal or noise components (most significantly, their distribution functions), appears in the literature describing nerve signal recordings from cuff-electrodes. It is especially important that both a *spectral* and *distribution* characterization be performed on the noise component(s) alone. Given certain, valid, assumptions about the noise character (i.e., white, Gaussian, stationary, etc.), it may be feasible to design detectors which are highly robust (insensitive to additive noise).

Manuscript received July 26, 1996; revised December 8, 1997 and March 9, 1998. This work was supported by The Danish National Research Foundation, The Danish Foundation for Physical Disability, and The Danish Ministry of Industry.

The authors are with the Center for Sensory-Motor Interaction, Aalborg University, Aalborg DK-9220 Denmark.

Publisher Item Identifier S 1063-6528(98)03849-X.

Although these processing methods are flexible enough to be useful in a variety of neural prosthetic applications, we have chosen to limit our attention to one, namely correction of "drop-foot" in a hemiplegic human subject. Drop-foot, characterized by the inability of the subject to achieve adequate dorsiflexion of the foot to facilitate normal gait, has been successfully remedied via electrical stimulation of the *peroneal* nerve, [12]. In addition, previous work has demonstrated that afferent nerve signals recorded via nerve-cuff electrodes, can replace the heel switch (artificial sensor), traditionally used to control the stimulator in synchrony with the gait phase, [1]. This work also provided us with an insight into the potential shortcomings of neural signal-based prostheses, especially when using analog RBI processing alone.

II. Methods

A. Nerve Signal Recordings

Afferent nerve signal recordings were obtained from the *calcaneal* nerve of a 42-year-old, male, multiple sclerosis patient, who suffers from a "drop-foot." This nerve contains strictly sensory afferent fibers, primarily innervating the heel area of the foot. Using local anesthesia, a nerve-cuff electrode, constructed from a 3-cm long section of biocompatible silicone tubing, was implanted approximately 5 cm proximal and 3 cm posterior to the medial malleolus of the left ankle joint, [13]. The chronic implantation of this electrode for the purpose of recording nerve signals was approved by the local medical ethics committee. Five deinsulated, multistranded stainless steel wires serve as the nerve/electrode interface in this silicone cuff (where three were used at a time, connected in a standard "tripolar" configuration), [4]. The wires from this cuff were routed subcutanously across the *triceps surae* muscles, to an exit site approximately 30 cm above the lateral malleolus. The proximity of the cuff electrode to these muscles, and, possibly, a lower cutaneous receptor density within the innervated area, resulted in SNR's that were lower than seen in previous nerve-cuff recordings from the *sural* nerve, used in [1]. Nerve signal recordings were collected during gait (with both stimulation assisted and voluntary dorsiflexion), both with and without footwear, over a period of six months. In an attempt to record "pure" neural activity (without EMG contamination), recordings were also made during which a 2-cm (diameter) strain-gauge instrumented probe was used as a manipulandum, providing artificial mechanical cutaneous stimuli to the sedentary subject (see [10] for details). However, as is evident in Fig. 1, despite the application of a significant mechanical stimulus, little change in the raw nerve signal is seen.

A limited sequence of previously recorded nerve-cuff electrode signals from a second patient, with a cuff electrode implanted on the sural nerve (innervating the dorsal and lateral pert of the foot [1]) were analyzed off-line. The results were comparable to the data shown herein.

All nerve-cuff electrode signals analyzed by the detection algorithms presented herein were preamplified by 100 dB (100 000×) using a transformer-coupled amplifier (Micro Probe, Inc. ADT-1), and processed in real-time (unless otherwise noted) by the DSP neural prosthetic system, with

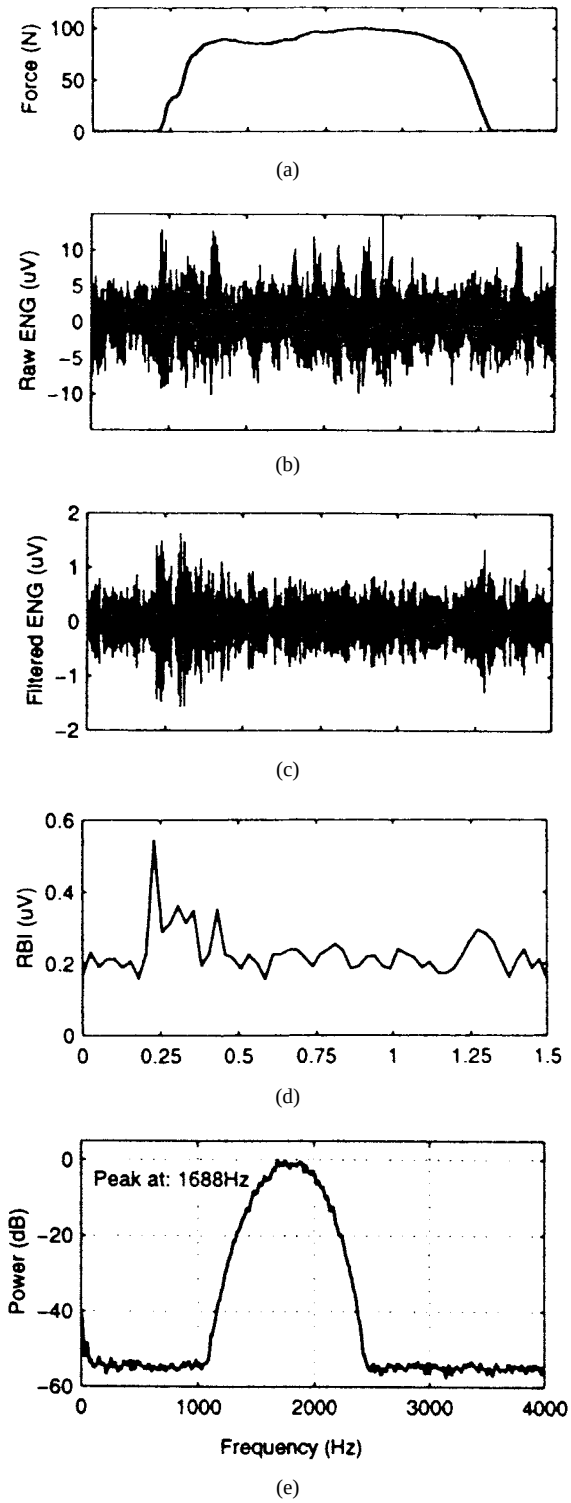

Fig. 1. (a) The perpendicular force (in Newtons) applied to the heel of the subject, who was relaxed, and sitting upright. (b) The unprocessed nerve signal recorded from the cuff electrode as a result of this mechanical stimulus. (c) The signal in (b) filtered by two ninety-first order FIR filters (1.6–1.9 kHz, −3 dB points), as implemented on the DSP. (d) The RBI signal resulting from applying (1) without a noise threshold on frames of 667 samples (corresponding to a 33-ms interpulse interval). Electrical stimulation was not used, so the window that would otherwise be specified by the stimulation pulses was simulated. (e) The power spectral density estimate (periodogram-based) of the filter applied in (c).

which they were amplified by an additional 6 dB. The raw and processed nerve signals, together with the output from a heel-contact switch placed in the subject's shoe (to serve as an independent "control" indicator of gait phase), were recorded both by computer (using an isolated serial interface between the DSP system and a standard IBM-compatible PC), and onto digital audio tape (DAT). The amplified nerve signal was over-sampled at a rate of 20 kHz, in order to minimize the effects of the A/D converter's anti-aliasing filters, and digitally decimated by the DSP.

B. Peroneal Nerve Stimulation

It was desirable that the subject's gait not be influenced by any potential detection errors, and that an algorithm independent reference signal be available for comparison. Therefore, the mechanical switch, placed in the subject's shoe, was used to control a custom-built, constant-current stimulator, turning it on/off during swing/stance phases (respectively). Surface stimulation electrodes (Axelgaard Ltd., PALS) were applied above the peroneal nerve, and a constant stimulation frequency (30 Hz, typically) utilized, with biphasic pulses ranging in width from 0 to 300 μs, and current from 10 to 40 mA. Current settings were adjusted before each trial to ensure that adequate stimulation-induced foot dorsiflexion was achieved. The pulse width was ramped up/down on stimulator activation/deactivation (respectively) to provide for more gradual foot motion, and reduce patient discomfort. Typically, electrode impedances of 1.5 kΩ were measured, resulting in maximum pulse amplitudes of 60 V.

C. Preprocessing

All processing methods employed in FES applications to date utilize a windowed sample of the recorded cuff electrode signal, where the number of samples in the window is a function of the sampling frequency, and the stimulation pulse rate, [14]. As a result of the high amplitude stimulation pulses applied to the skin, a large stimulation artifact voltage appears in the recorded cuff electrode signal. Although it has been suggested that measures should be taken to protect the preamplifier, and eliminate this artifact by "blanking," we have not found this to be necessary, [15]. Rather, since the DSP receives interrupting pulses synchronized to the stimulation pulses, it is possible to perform this blanking function in software. It should be noted that this approach requires that the saturation recovery time of the nerve-cuff electrode preamplifier is short ($<$1 ms). Thus, the first step in the processing, common to all algorithms, was the segmentation of the sampled nerve signal into windowed "bins," bounded in duration by the adjacent stimulation pulses (the *interpulse* interval). A stimulation frequency of 30 Hz (resulting in an interpulse interval of 33 ms) was typically used.

D. Filtering

The most important step in neural signal processing is, unquestionably, filtering of the "raw" signal. Results of both wavelet and Fourier analysis of raw (unfiltered) cuff signals indicate that, for the particular cuff electrode configuration used in these experiments, the most significant portion of neural signal energy lies in a narrow frequency band between 1.0–2.0 kHz, [16]. This has also been seen in experiments performed on animals, [10]. A variety of digital FIR filters were realized on the prototype DSP system, and a performance analysis performed on real nerve signal data. The optimization criterion selected was based upon the mean SNR's of the filtered RBI signals. Here, SNR was derived from the ratio of the mean RBI amplitude recorded whilst mechanically stimulating the subject's heel (with a perpendicular force of approximately 50N, using a strain-gauge instrumented, 2 cm diameter metal probe) to the mean RBI amplitude recorded during the absence of any mechanical stimulation. It was found that, although there is some nerve signal energy over 2.0 kHz, the SNR of the unfiltered signal in this band is low. Thus, the raw signal recorded above 2.0 kHz is dominated by thermal noise (from both the amplifier and electrode), whose power is proportional to the square-root of the bandwidth utilized. Although this noise follows a $1/f$ characteristic below 100 Hz, it appears to have a relatively constant power level above this frequency. Thus, an upper frequency cutoff limit can be derived by optimizing the tradeoff between (possibly) obtaining additional nerve signal energy using a higher cutoff frequency, and a reduction of the filtered signal's SNR due to the increased contribution of thermal noise in the high frequency band.

Consistent with previous results, a neural signal peak between 1.0 and 2.0 kHz was observed, [1]. Therefore, the lower frequency filter cutoff point can be obtained by optimizing another tradeoff: the rejection of interfering muscle (EMG) signal verses the incorporation of additional low-frequency nerve signal information. Although the EMG signal power falls off rapidly above 100 Hz, some measurable energy content may be present at frequencies as high as 1 kHz. In order to ensure that all EMG was eliminated in adjacent frequency bands, we used very high-order filtering, typically employing a cascade of ninety-first order FIR lowpass and highpass filters (designed using the Remez Exhange Method optimization of Chebyshev polynomials), with stop-bands below $-$90 dB, [17]. Fig. 1(e) shows the power spectrum (recorded from the D/A output of the DSP system, digitized to 12-bits, using a 20 000 Hz sampling frequency). It is important to note that, at 1.0 kHz, the filtered signal power corresponds to the quantization noise floor of the D/A converter (which is near the numerical accuracy limit of the DSP itself). Thus, all deterministic signal components are removed below this frequency (and above 2.5 kHz).

Despite the evidence of a nerve signal peak near 1.0 kHz, a filter bandwidth of 1.6–1.9 kHz ($-$3 dB) proved to yield the highest SNR (most consistently) when comparisons were made using a variety of empirically selected filters to process a random nerve signal test set, representing over 600 gait cycles. This may be attributable to two factors: 1) The mean EMG noise power is typically below the mean nerve signal power at 1.6 kHz and 2) a significant portion of the real-time tests were performed using only half of the five-pole cuff (i.e., an effective cuff length of 1.5 cm). This was necessary since, two months after implantation, two of the

lead wires to the cuff-electrode began to fail (as indicated by abnormally high impedance measurements). Thus, the nerve signal frequency content (which has been shown to follow an inverse relationship with electrode length, [4]) peaked, as expected, at a correspondingly higher frequency. A final consideration regarding the filtering operation, concerns the ordering of the cascaded lowpass and highpass stages. In order to smooth some of the high frequency oscillations induced by the abrupt signal amplitude changes (spikes) passing through the A/D's antialiasing filter, the nerve signal was always low-pass filtered first.

After the preprocessing and filtering steps were performed, the resulting signal was processed by one of the algorithms described in Section III. The preprocessed signal (and the real-time processed output in the case of the RBI algorithm) was then recorded digitally (as a 16-bit value), and converted to analog form (0–3 V, 14-bit resolution) for storage onto DAT. An analysis of the detection accuracy of the processed signals was performed off-line, by comparing the heel switch data with the digital recording of the detector's output using a random selection of over 300 complete gait cycles, recorded on different days.

III. Processing Algorithms

Once the primary energy content of the nerve signal has been isolated via the windowing and filtering operations, activity in response to mechanical skin stimuli becomes more apparent, as indicated in Fig. 1(c). Typically, the SNR's of the preprocessed signals lie in the range of 0 dB to $+3$ dB. Given that changes in signal amplitude of the preprocessed signals are evident to the eye, it is logical to investigate the feasibility of a simple detection algorithm utilizing these changes. Thus, we proceeded in three steps, in the direction of increasing algorithmic complexity, progressing from "analog-like" RBI processing, to statistical signal processing methods, restricted to digital domain realizations.

A. Rectified and Bin-Integration

After the low-pass and high-pass filtering operations have isolated the principal neural signal energy band, the simplest real-time algorithm employed (Rectified Bin wise Integrations) requires that a standard vector *p-norm* be computed. Both the "1-norm" (the digital analogy to the analog integration method), and the squared, or "2-norm" (usually referred to as "short-time energy") were computed. In practice, little performance difference was seen between these two norms. In order to retain backward compatibility with a simple analog implementation (although an analog "squaring" circuit is a viable option), we chose to use the 1-norm. This is computed once for each interpulse frame, using all L samples in the interval, where L is determined by the ratio of the sampling frequency f_s, and the stimulation pulse frequency, f_{stim}. For typical values, $L = 667$ samples. In order to reduce the effects of the additive noise on the integrated result, a *fixed*, empirically determined noise *threshold*, T_n is specified. Only the portion of the signal amplitude which *exceeds* this threshold (in absolute value) is included in the integrated result. It is interesting to note that a similar metric, the Willison Amplitude (in which only *changes* in successive samples, which exceed a given threshold, contribute to the integration), has been successfully applied to EMG analysis, [18].

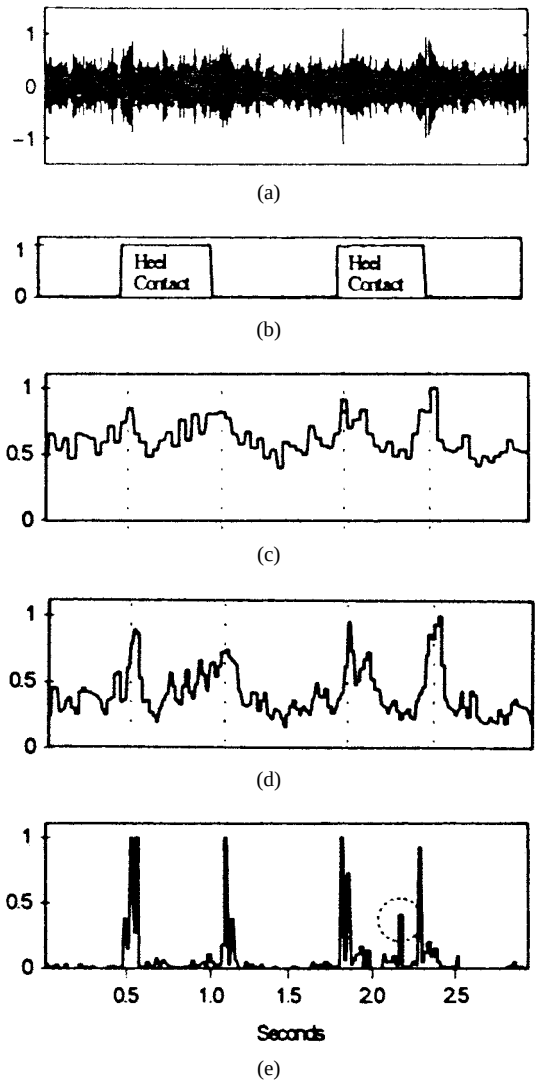

Fig. 2. (a) The filtered (1.6–1.9 kHz) nerve signal recorded during stimulation assisted gait. (b) The output from the heel switch, where a high level indicates that the heel is loaded (during stance phase). (c) The output of the RBI algorithm, processed in real-time on the DSP system. (d) and (e) The outputs of the second and third-order algorithms (respectively), processed off-line. Note that, although the third-order algorithm approaches the ideal output (a burst of activity corresponding to *changes* in the applied mechanical stimulus, in this case, heel contact/lift events), it also suffers from false positives (FP's). One such FP, corresponding to an erroneous detection of heel-lift, is circles. The increase in peak to average ratio (PAR) values [see (8)] in moving from RBI, to second and third-order algorithms is also evident here, as seen by the increased difference between the output during swing phase (the noise-only case), and the peak outputs during contact/lift events.

Fig. 2(c) indicates the results obtained using a real-time (DSP) implementation of this digital RBI algorithm, applied during stimulation assisted gait. Most striking, is the small difference between the peak values (corresponding to neural activity events), and the nominal value, indicating the relatively narrow range of threshold settings which yield high detection percentages. This is a significant drawback of all

p-norm detection algorithms, which are based solely upon the first-order statistical properties of the analyzed signal.

B. Subspace Decomposition Methods: Principles

The most significant problem with a simple p-norm measure is that there is no decomposition of signal and noise subspaces. Both signal and noise contribute with equal weighting to the result. While not important when operating with high SNR signals, it is a significant shortcoming in this application. Several methods, generally know as *super-resolution* algorithms, have been proposed, with which it is possible to separate the signal and noise subspaces, [8]. The general idea behind these algorithms can be expressed as follows.

- If the autocorrelation matrix of an *ideal* white-noise (fully uncorrelated) process is formed, only the diagonal entries (indicating zero time delay or "lag") will be nonzero, corresponding, in fact, to the variance of the noise.
- The eigenvectors of the correlation matrix of any, general process, provide a measure of the *principal components*, or information content of this process, where the eigenvalues indicate the relative importance of these components.
- These eigenvalues are determined through a transformation which *diagonalizes* the correlation matrix, and correspond to the resulting diagonal elements. One such method is the application of a singular value decomposition (SVD).
- Since the correlation matrix of a noise process is already diagonal (where all elements are equal, representing the noise variance), any general vector is an eigenvector, and only a *single*, repeated eigenvalue is obtained. Thus, as expected due to its random nature, there is no structure or information content in such a process. However, when a deterministic *signal* component is present, different eigenvalues result, where the *spread* (difference) between the largest (one or few) and smallest can be used to provide a measure of the amount of information content present.

It is assumed that the smallest eigenvalue represents only noise, and the largest the most significant of the principal components, where an ordering of eigenvalues represents an optimal (in a least-squared sense) partitioning of signal energy content. This general principle has been successfully employed to denoise/compress speech data via the Karhunen–Loéve Transform, and similar SVD-based methods, [19].

C. Autocorrelation-Based (Second-Order) Processing

For zero mean signals, their covariance (second-order moment) and autocorrelation functions are identical. The autocorrelation matrix of data frames output from the preprocessing operations (of which the high-pass filter ensures zero mean signals) can be coupled with an SVD algorithm to implement a subspace decomposition algorithm as outlined as follows.

1) The Toeplitz matrix $\boldsymbol{R}$ is formed using an *estimate* of the autocorrelation function

$$r(\tau) = \frac{1}{L}\sum_{n=0}^{L-1} x(n)x(n-\tau), \text{ where } L \text{ is the frame length.} \quad (2)$$

Here, wide-sense stationarity is assumed, so only the values of $r(\tau)$ for *positive* lags need be computed (due to symmetry). A subset of Q of these L values of $r(\tau)$ where Q is chosen empirically (typically $Q = 10$), is then arranged in $\boldsymbol{R}$ as

$$\boldsymbol{R} = \begin{bmatrix} r(0) & r(1) & \cdots & r(Q-1) \\ r(1) & r(0) & \cdots & r(Q-2) \\ \vdots & \cdots & \ddots & \vdots \\ r(Q-1) & \cdots & r(1) & r(0) \end{bmatrix}. \quad (3)$$

2) A singular value decomposition is performed on $\boldsymbol{R}$, yielding its eigenvalues

$$\boldsymbol{U}^T\boldsymbol{R}\boldsymbol{V} = \Sigma, \text{ where } \boldsymbol{U} \text{ and } \boldsymbol{V} \text{ are unitary matrices} \quad (4)$$

and Σ is a diagonal matrix $\Sigma = \text{diag}(\sigma_1, \sigma_2, \cdots, \sigma_M)$, in which the singular values, σ_n, correspond to the absolute value of the eigenvalues of $\boldsymbol{R}$. However, since $\boldsymbol{R}$ is *positive definite*, its eigenvalues are all positive and no information is lost.

3) The difference d between the largest and smallest eigenvalues is computed, and compared against an empirically determined threshold, T_d

$$d \equiv \sigma_{\max} - \sigma_{\min} \underset{H_0}{\overset{H_1}{\gtrless}} T_d, \quad \text{where } H_0 \text{ indicates the null hypothesis} \quad (5)$$

(noise-only) and H_1 indicates the presence of signal in noise.

A representative output (where the eigenvalue-spread d is plotted) resulting from the application of this algorithm during stimulation assisted gait (for drop-foot correction) is shown in Fig. 2(d).

D. Cumulant-Based (Third-Order) Processing

Higher order spectra (HOS) have shown great promise recently when used to implement robust detectors of signals contaminated with high levels of noise, [9]. These exhibit a number of desirable properties which enable ideally the separation of signal and noise subspaces, [20]. These are largely due to the inherent properties of Gaussian processes, most significantly, that all information about such processes is contained in their first two moments, [21]. Thus, higher ordered moments evaluate to zero for ideal Gaussian processes, a typical example of which is thermal noise. Conceptually then, such noise ideally can be completely separated from a non-Gaussian process (signal) using a subspace decomposition method similar to that employed with the second-order method, but using a third- (or higher) order statistic, typically referred to as a *cumulant*. In order for a HOS-based decomposition to be efficiently employed, a number of assumptions regarding the nature of the signal to be detected, and the contaminating noise must hold. Most significantly, the probability density function (pdf) of the noise must follow a Gaussian (normal) distribution, while the pdf of the signal of interest must be significantly divergent from a normal distribution. Also, the noise must be additive, and uncorrelated with the signal.

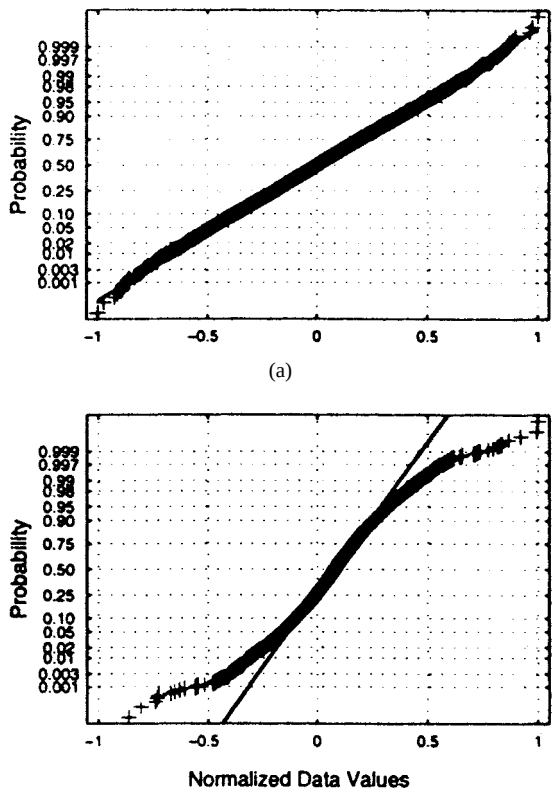

Fig. 3. Normal quantile–quantile plots, comparing the distribution functions of the tested signals with a Gaussian distribution (indicated by the diagonal lines). Distribution of sections of filtered data (10 000 samples) recorded during, (a) swing phase (noise-only), and (b) stance phase (signal+noise).

It should be emphasized that, although the original (unprocessed) noise appears to be nearly white (except at very low frequencies, where the amplifier's $1/f$ noise is significant), and normally distributed, any nonlinear processing operation performed (filtering, for example), has the potential to change both its spectral and distribution properties. The preprocessing filters applied are no exception. Thus, the suitability of HOS methods must be verified by examining representative samples of preprocessed data.

Assumptions regarding the distributions of the signal and noise components can often be confirmed (or rejected) using *normal quantile-quantile* plots, [22]. Fig. 3 shows such a plot of the distributions (relative to a normal distribution) of a section of "noise-only" data recorded from the nerve-cuff electrode during swing phase, and a section of data from the immediately following stance phase in which neural activity is present. It is clear that there is a marked difference in the distributions of the noise-only and signal + noise data samples. Whereas the noise-only section appears to adhere well to the expected normal distribution, the signal+noise section exhibits a clear "tailedness" (symmetric divergence from a Gaussian distribution).

A quantitative measure of the statistical properties depicted in these plots can be obtained through the use of the Kolmogorov–Smirnov (K–S) test, which measures the overall difference between two cumulative distribution functions (cdf), [23]. The K–S values comparing the distributions of noise-only and signal + noise sections of a nerve signal recording (the same as displayed in Fig. 1) are shown in Table I. When a segment in which nerve signal activity is present is compared with a noise-only segment, the large K–S value resulting from the test serves to reaffirm the likelihood that a statistical signal detection algorithm, which is sensitive to deviations in distribution functions, will be applicable.

TABLE I

VALUES OF THE K–S TEST APPLIED TWO SIGNALS. THE 95% CONFIDENCE LEVEL THAT THE SIGNALS HAVE THE SAME DISTRIBUTION FUNCTION (cdf) IS INDICATED BY A K–S VALUE OF 0.035. THE GAUSSIAN/GAUSSIAN CASE IS INCLUDED AS A MEANS OF VERIFYING THE ACCURACY OF THE IMPLEMENTATION. IN THIS CASE, TWO SIGNALS WHICH SHOULD HAVE IDENTICAL (NORMAL) cdf's WERE COMPUTER GENERATED. WHEN TWO SEPARATE, NOISE-ONLY (NO NEURAL ACTIVITY WAS EXPECTED DUE TO A LACK OF MECHANICAL STIMULATION) SECTIONS OF RECORDED NERVE DATA ARE COMPARED, THE K–S VALUE INDICATES THE LIKELIHOOD THAT THEY ARE, INDEED, IDENTICALLY DISTRIBUTED. THIS ALSO HOLDS WHEN TWO RECORDINGS WITH APPRECIABLE NEURAL ACTIVITY ARE COMPARED. THE LARGE K–S VALUE SEEN WHEN A SIGNAL + NOISE SECTION IS COMPARED WITH AN IMMEDIATELY ADJACENT NOISE-ONLY SECTION, INDICATES A SUBSTANTIAL DIFFERENCE IN THEIR DISTRIBUTION FUNCTIONS. THIS DIFFERENCE CAN BE THOUGHT OF AS BEING ANALOGOUS TO THE DIFFERENCE IN MAXIMUM EIGENVALUES COMPUTED WITH THE THIRD-ORDER ALGORITHM

Signal #1	Signal #2	K-S Value
Gaussian	Guassian	0.018
Noise-only	Noise-only	0.029
Signal+noise	Signal+noise	0.027
Signal+noise	Noise-only	0.119

An algorithm which is sensitive to deviations from a normal distribution, in analogy to the second-order method, can be developed using a time-domain metric of the value of the third-order cumulant of the preprocessed nerve signal, by performing the following steps.

1) A Toeplitz matrix is formed using an *estimate* of the third-order cumulant of a data frame.
2) The largest eigenvalue $\lambda_{\max}$ of the Toeplitz matrix is computed. Although the SVD method employed in the second-order algorithm could be used, it is more efficient (computationally) to use a power iteration which yields *only* the maximum eigenvalue [24].
3) This value is compared against an empirically determined threshold, T_λ

$$\lambda_{\max} \underset{H_0}{\overset{H_1}{\gtrless}} T_\lambda, \text{ where again } H_0 \text{ indicates the null hypothesis} \quad (6)$$

(noise-only) and H_1 indicates the presence of signal in noise.

The results of the application of this algorithm are shown in Fig. 2(e). Here, the increase in the SNR of the signal applied to the threshold detection algorithm, corresponding to the effective range of threshold values for which valid detections are made, is noteworthy. The practical effect of the separation of signal and noise subspaces is evident in the significantly reduced noise "floor" during noise-only sections.

IV. RESULTS

A quantitative performance index which we term the peak-to-average ratio (PAR), was calculated for the outputs of each

algorithm, using the recorded heel-switch data. It is defined as

$$\mathrm{PAR} = 20\log\left(\frac{\sum_{K}\max(S_{\mathrm{Event}})}{\sum_{K}\sum_{i=1;L}x_i}\right), \quad \text{with}$$

$$S_{\mathrm{Event}} = \left\{x_{H-i},\cdots,x_{H+i} : x_H \in H_1, i = \frac{p}{2}.\right\} \qquad (7)$$

Here, S_{Event} corresponds to the set of m algorithm output values which occur during a window of width Δp samples around sample x_H where a valid neural event is *expected* (as determined from the heel-switch data). The average over K gait cycles of the *maximum* output value within this window is computed, and compared to the average algorithm output (across all L samples in each of the K cycles). Typically, p was selected to provide a window width of 100 ms (where it was assumed that a timing error of less than ± 50 ms in the detection of a heel transition would not be noticeable in a drop-foot correction prosthesis). The PAR value is illustrative in comparing the results of the three algorithms. The RBI algorithm yielded an average ($\pm$std. dev.) PAR value of 5.1 $\pm$ 0.8 dB. The second and third-order algorithms resulted in average values of 8.5 $\pm$ 1.4 and 20 $\pm$ 2.8 dB, respectively. The PAR value also provides a measure of the detector's sensitivity to algorithm parameters when a simple threshold comparator is applied, where PAR then is an indicator of the ability of a detection algorithm's immunity (evident as a constant detection percentage) to nonstationarities in both signal and noise power.

The theoretically reduced sensitivity of the second- and third-order methods to additive noise is shown in Fig. 4 to be of practical value when processing nerve-cuff electrode signals. Here, the output of the three detectors having processed a typical nerve signal with a single activity burst resulting from mechanical stimulation with a metal probe is shown. However, starting at sample number 7000 (a "noise-only" stretch), the "gain" of the nerve signal is linearly increased from 0 dB (no amplification) to +6 dB (2× amplification). If the outputs during the period of true neural activity (around sample number 4000) are considered, the results of each algorithm when processing signals of various SNR's (ranging from approximately +3 to 0 dB), can be simulated. As the SNR decreases, the RBI algorithm becomes less effective (as indicated by the linear increase in its output values), while both the second- and third-order methods are substantially less influenced.

A comparison of the average *detection* ability of the RBI, second-order eigenvalue-spread and third-order algorithms, having processed more than 300 step cycles is presented in Fig. 5. Here, the detection percentages shown are in relation to a 100% standard derived from the heel-switch data (where gait cycles during which the switch erred, typically 2–3% of the total, were deleted). These percentages represent the ratio of the number of true detections (detections minus false positives, FP's) to the number of possible heel contact/lift events, as registered by the corrected heel-switch data. A

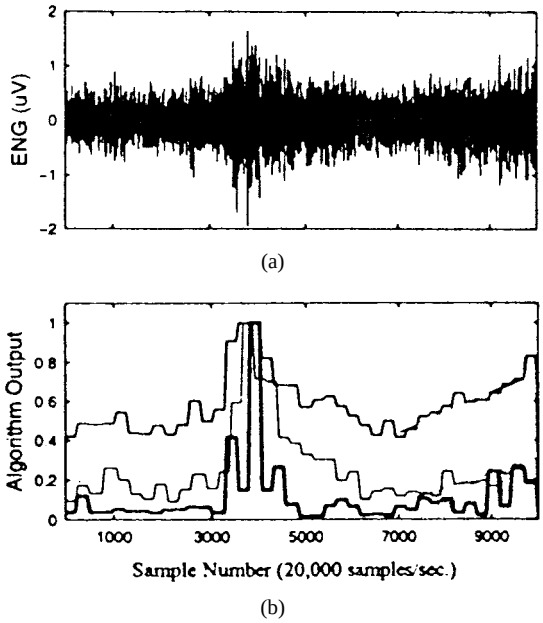

Fig. 4. (a) The filtered (1.6–1.9 kHz) nerve signal (10 000 samples) resulting from a single mechanical stimulation with a metal probe (contact occurs just past 3000 samples). The artificially increased amplitude, ramping up from samples 7000 to 10 000, is also evident. (b) The output of the three algorithms in response to (a). The medium-weight line (top trace) shows the RBI output, the light-weight line the second-order output, and the thick line (bottom trace) the third-order output.

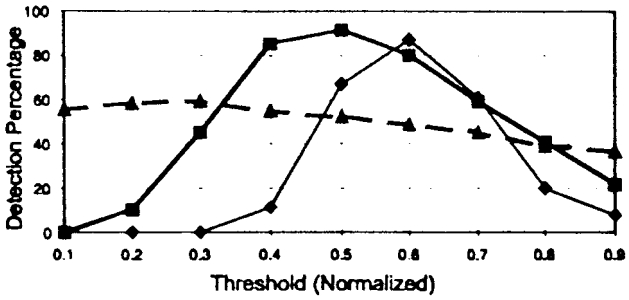

Fig. 5. Heel contact detection percentages for the three algorithms (using a simple threshold detector). Thin continuous line is the rectification and windowed (bin)-integration (RBI). Heavy continuous line is the second order and broken line is the higher order spectra (HOS) statistical signal detection algorithms.

range of threshold values (for a simple, threshold detector) was determined for each of the three algorithms, ranging from zero, up to the maximum output value (different for each algorithm). This range was then normalized for comparative purposes. In calculating the shown detection percentages, equal weighting was given to FP's and missed-detections. Thus, the peak values shown here correspond to the optimal threshold value selected by the Bayes criterion (minimizing the average error cost), [25].

It is important to observe that the second-order detector exhibits a substantially lower dependence upon threshold settings. Although the *peak* detection rates of the RBI and second-order algorithms are similar, the high sensitivity of the RBI method to the detection threshold setting is evident through the rapid decrease in detection percentage when operating with nonoptimal thresholds.

V. Discussion

Although it is evident (Fig. 5) that the statistical signal processing methods advocated improve the insensitivity to a simple threshold detector, the question as to whether or not this improvement is *functionally* significant in an FES application must be posed. This, largely, depends upon the success with which the detection threshold setting applied to the RBI algorithm's output can be optimally adjusted. Both the results from this study, and that described in (1) indicate that finding the optimal threshold is not a trivial task. Furthermore, it should be noted that both the second- and third-order methods were able to detect some individual events that were not detected by the RBI method. If such an event is surrounded by events otherwise easily detected, then its functional significance is much greater than indicated by the *small* increase in the average detection percentage. The true worth of these methods must be measured under "real-world" conditions, where signal parameters are nonstationary, and it cannot be assumed that a specific, fixed threshold value is optimal. This issue can be addressed for each algorithm in turn:

A. RBI Algorithm

The improvement in SNR obtained through the digital implementation can be attributed, primarily, to the improved filtering available in the digital domain, and, to a lesser extent, to the greater precision of digital integration and rectification, and the incorporation of a "noise threshold" into the standard RBI algorithm. A spectral analysis of EMG and nerve signal components resulting from the low-order analog filters in the previously developed analog processing system indicated the likelihood of EMG contamination (i.e., incomplete separation) during a significant portion of this interpulse period, [1]. The solution employed was to simply delay nerve signal processing until the majority of the contaminating EMG component had died away, late into the interpulse window. Unfortunately, a significant portion (over 65%) of useable nerve signal data is thereby lost. Additionally, it could not be conclusively maintained that no EMG contamination contributed to the resulting "nerve-only" signal. Despite the digital RBI implementation's improved utilization of the nerve signal by virtue of high-order filtering, the sensitivity of this first-order method to noise remains.

One possible solution would be the coupling of an adaptive detector threshold level determination algorithm. Although conceivable, we suspect that such a system would be difficult to implement in practice, given the potential for variations in nerve signal energies on a cycle-by-cycle basis, due to different foot contact patterns during gait. In addition, a "training" session would be required periodically, in which the RBI algorithm's performance relative to a known control (a heel-contact switch, for example) could be monitored, and the *initial* threshold value optimized. It seems likely that, given the substantially improved ability of the second-order algorithm to achieve high detection percentages despite large variations in threshold values, such a detection threshold adaptation method would be more successfully applied there.

B. Autocorrelation (Second-Order) Algorithm

Although the second-order algorithm should, ideally, be completely immune to additive white noise, this desirable property was not seen when processing very noisy, real nerve signals. This might indicate that, either, the "coloring" of nerve signals is sufficiently nonwhite such as to invalidate the assumptions, or the number of samples and lags used were insufficient to provide a valid estimate of the true autocorrelation function. When a simulated nerve signal (a white, Gaussian noise background with a simulated neural event consisting of a burst of band-limited white, Gaussian noise) was processed, near ideal results were obtained with SNR's as low as 0 dB. This served both to verify that the algorithm was implemented properly, and to indicate the difficulties in developing a truly accurate model of real nerve signals.

C. Higher Order Statistical (Third-Order) Algorithm

The high false positive rate which contributes to low, overall, detection percentages when using the third-order detector can likely be attributed to two factors: 1) some neural activity may, in fact, be present, when an FP detection is assumed and 2) the statistical distribution of nerve signals recorded by the cuff electrode in this application may result in the unsuitability of a metric based upon their third-order statistical properties alone. Specifically, their skewness may, on average, be too small to be reliably detected. The first issue is more difficult to address. Here, although the detection algorithm may be "optimal" in the sense that it is highly accurate in detecting *true* neural events, it may not be functional when utilized in this particular application. It is likely that small perturbations during swing phase (skin stretching, mechanical stimulation due to skin/shoe contacts, etc.), which might give rise to detectable neural activity, must be rejected by other means.

The second problem can, possibly, be solved using a different HOS-based metric. Given the stationary noise statistics exhibited, information obtained from a noise-only section of data (via computation of its covariance matrix) can be used to further improve the reliability of the third-order detector, as well as to provide for an automatic, statistically significant determination of the threshold level required to ensure a bounded (specified) false positive rate. In this case, the maximum eigenvalue is not used as a metric, but, rather, a matrix product, normalized by the covariance matrix, is computed, [26]. Future improvements to the HOS (third-order) algorithm are also likely to be achievable through the use of a frequency domain analysis of the cumulant values. A two dimensional, complex, Fourier transform of these values, termed the "*bispectrum*," has been shown to provide additional information in other applications, [27].

An analysis of the recorded nerve signal indicates that it often follows a symmetrical, non-Gaussian distribution (see Fig. 3). The third-order cumulant analysis performed is, ideally, insensitive to *perfectly* symmetrical distributions. Thus, it is possible that a fourth-order (trispectrum) analysis, which provides a measure of the *kurtosis* (curvature) of a distribu-

tion function, may improve the results. Simple fourth-order methods have been successfully applied when signals are symmetrically, yet not normally distributed, [28]. We are presently investigating potential real-time applications of such fourth-order methods.

D. Detection Algorithms

It may also be feasible to improve the overall detection accuracy by applying more advanced (than a simple threshold comparator) postprocessing on the algorithm outputs. It should be noted that a "worst case" analysis was performed in determining the detection percentages presented. No *a priori* knowledge of the human gait cycle was assumed. Thus, many false positives which occurred in swing phase *could* have been rejected by applying an exclusion rule over a window in which contacts are unlikely to occur (i.e., near the middle of swing phase). Alternatively, adaptive logic network (ALN), using the same, preprocessed RBI data described here can be used. Preliminary analysis has already shown promise, [29]. Although ALN's are particularly suitable for simple, digital implementations (being based on logic and delay operations only), the single-cycle multiply-accumulate facilities of DSP IC's allow for straight-forward implementations of traditional neural network structures as well.

E. Real-Time Implementation Issues

The use of a relatively low-power, fixed-point DSP has proven to provide an acceptable compromise between processing ability and power consumption, indicating that a fully implanted, all digital processing system is feasible. Still, it should be noted that the subspace decomposition methods described require a substantially larger number of computations than the RBI algorithm. In addition, all standard implementations of SVD and eigenvalue solvers require floating-point computational accuracy. This is a significant problem, when real-time, *low-power consumption* implementations are being considered. Typically, floating-point signal processors consume several times (at least a factor of ten) more power than their fixed-point counterparts, eliminating them from consideration when selecting potentially implantable hardware. Thus, the conflicting requirements for precision, power consumption, and processing speed must be tradedoff. To this end, some portions of an algorithm can be implemented in software simulated floating-point, at the expense of speed, although, finding an optimal balance is difficult. Therefore, at the time of this writing, the second- and third-order algorithms have only been fully implemented in nonreal-time simulations, using low-precision (16-bit) floating-point arithmetic. However, based upon the results of these simulations, we do not see any fundamental hindrance to the development of a real-time realization in the near future.

VI. Conclusions

We have investigated the ability to detect the presence of afferent nerve signal activity recorded by implanted nerve-cuff electrodes in a very noise environment through the application of digital signal processing methods in implementing subspace separation algorithms, based on the second- and third-order statistical properties of these signals. An analysis of their statistical distributions indicates that there is a significant (i.e., detectable) difference between the noise-only and signal + noise cases, confirming the viability of these statistical signal processing methods. In addition, the improvements in filtering obtainable in the digital processing domain have also proven to be an important first step in increasing detection reliability. Although still coupled to a simple threshold comparator, the insensitivity to algorithm parameters of these advanced algorithms is substantially greater than that of the traditionally applied first-order metric (RBI). Various portions of the algorithms discussed have already been implemented in real-time, DSP-hosted form. In addition, simulation results indicate that it is feasible to implement the complete algorithms presented here on the presently developed, fixed-point DSP-based neural prosthetic system.

Acknowledgment

The authors would like to thank Dr. M. Haugland for constructing the nerve-cuff electrode and Chief Neurosurgeon J. Haase (Aalborg Hospital) for implanting it. Special thanks go to Dr. M. Rangoussi (with the National Technical University of Athens), for an excellent explanation of her Ph.D. work on HOS detection algorithms.

References

[1] M. Haugland and T. Sinkjær, "Cutaneous whole nerve recordings used for correction of footdrop in hemiplegic man," *IEEE Trans. Rehab. Eng.*, vol. 3, pp. 307–317, Dec. 1995.

[2] A. Lickel, "Restoration of lateral hand grasp in a tetraplegic patient applying natural sensory feedback," Ph.D. dissertation, 1998, pp. 1–120.

[3] J. Hoffer, "Techniques to record spinal-cord, peripheral nerve, and muscle activity in freely moving animals," in *Neurophysiological Techniques: Applications to Neural Systems, Neuromethods 15*, A. Boulton *et al.*, Eds. Clifton, NJ: Humana Press, 1990, pp. 65–145.

[4] R. Stein, D. Charles *et al.*, "Principles underlying new methods for chronic neural recording," *Le J. Canadien Des Sci. Neurol.*, Aug. 1975, pp. 235–244.

[5] K. Johnson *et al.*, "Perspectives on the role of afferent signals in control of motor neuroprostheses," *Med. Eng. Phys.*, vol. 17, no. 7, pp. 481–496, 1995.

[6] M. Thomsen, J. Struijk, and T. Sinkjær, "Nerve cuff recording with a combined mono- and bi-polar electrode," *IEEE Trans. Rehab. Eng.*, to be published.

[7] A. Metting van Rijn, A. Peper, and C. Grimbergen, "High-quality recordings of bioelectric events," *Med. Biologic. Eng. Comput.*, July 1991.

[8] S. Haykin, *Adaptive Filter Theory Second Edition*. Englewood Cliffs, NJ: Prentice Hall, 1991.

[9] M. Rangoussi, S. Bakamidis, and G. Carayannis, "On the use of SVD and high-order statistics for endpoint detection of speech," in *Levels in Speech Communication: Interactions and Relations*, J Schoentgen, Eds. Brussels, Belgium: Elsevier, 1995.

[10] M. Haugland, A. Hoffer, and T. Sinkjær, "Skin contact force information in sensory nerve signals recorded by implanted cuff electrodes," *IEEE Trans. Rehab. Eng.*, vol. 2, pp. 18–28, 1994.

[11] M. Zardoshti, B. Wheeler, K. Badie, and R. Hashemi, "EMG feature evaluation for movement control of upper extremity prostheses," *IEEE Trans. Rehab. Eng.*, vol. 3, Dec. 1995.

[12] P. Strojnik, R. Acimovic *et al.*, "Treatment of drop foot using an implantable peroneal underknee stimulator," *Scand. J. Rehab. Med.*, vol. 19, pp. 37–43, 1987.

[13] B. Upshaw and T. Sinkjær, "Real-time digital signal processing of electroneurographic signals," in *Proc. IEEE EMBS Conf. 1994*, 1994, pp. 1023–1026.

[14] ———, "Natural versus artificial sensors applied in peroneal nerve stimulation," *J. Artificial Organs*, vol. 21, no. 3, pp. 227–231, 1997.

[15] M. Haugland and A. Hoffer, "Sensory nerve signals recorded by implanted cuff electrodes during functional electrical stimulation of nearby muscles," *IEEE Trans. Rehab. Eng.*, vol. 2, pp. 37–40, 1994.
[16] Z. Nikolic, D. Popovic *et al.*, "Instrumentation for ENG and EMG recordings in FES systems," *IEEE Trans. Biomed. Eng.*, vol. 41, no. 7, pp. 703–706, 1994.
[17] P. Slot, R. Riso, and T. Sinkjær, "Time-frequency analysis of mechanically evoked ENG," in *Proc. IEEE EMBS Conf. 1996*, Amsterdam, The Netherlands, 1996, no. 5.7.5–6, p. 110.
[18] R. Willison, "A method for measuring motor unit activity in human muscle," *J. Physiol.*, vol. 168, pp. 35–36, 1963.
[19] C. Rorabaugh, *Digital Filter Designer's Handbook*. New York: McGraw-Hill, 1993.
[20] S. Jensen *et al.*, "Reduction of broad-band noise in speech by truncated QSVD," *IEEE Trans. Speech Audio Processing*, vol. 3, Nov. 1995.
[21] J. Mendel, "Tutorial on higher-order statistics (spectra) in signal processing and system theory: Theoretical results and some applications," *Proc. IEEE*, vol. 79, pp. 278–305, Mar. 1991.
[22] C. Nikias and A. Petropulu, *Higher-Order Spectra Analysis*. Englewood Cliffs, NJ: Prentice Hall, 1993, pp. 7–122.
[23] StatSoft, Inc., *Statistica for Windows (Volume II)*, 1995, p. 2697.
[24] W. Press, S. Teukosky, W. Vettering, and B. Flannery, *Numerical Recipies in C: The Art of Scientific Computing*. Cambridge, U.K.: Cambridge University Press, 1992.
[25] G. Golub and C. VanLoan, *Matrix Computations*, 2nd ed. Baltimore, MD: Johns Hopkins University Press, 1989.
[26] R. McDonough and A. Whalen, *Detection of Signals in Noise, Second Edition*. New York: Academic, 1995.
[27] M. Rangousse and G. Carayannis, "Adaptive detection of noisy speech using third-order statistics," *Int. J. Adapt. Contr. Sig. Processing*, Special Issue on HOS, Dec. 1995.
[28] L. Pflug, P. Jackson, J. Ioup, and G. Ioup, "Moment analysis of ambient noise dominated by local shipping," in *Proc. 8th IEEE Workshop Statistical Signal Array Processing*, 1996, pp. 271–274.
[29] A. Koskov, T. Sinkjær, and B. Upshaw, "Gait event discrimination using ALN's for control of FES in foot-drop problem," in *Proc. IEEE EMBS Conf. 1996*, Amsterdam, The Netherlands: Available only on CD-ROM, 1996.

Barry Upshaw received the B.Sc. degree in electrical engineering from the University of Santa Clara, CA, in 1985 and the M.Sc. degree in biomedical engineering from the University of Aberdeen, Scotland, in 1992. He is currently pursuing the Ph.D. degree at the Center for Sensory-Motor Interaction (SMI), the Department of Medical Informatics and Image Analysis at Aalborg University, Denmark.

His research is within the development of digital signal processing (DSP) systems for use in real-time, closed-loop control of functional electrical stimulation systems using natural bio-electric signals. His working interests at SMI include functional electrical stimulation systems, neural prostheses, and digital signal processing of bio-electric signals.

Thomas Sinkjær (M'84) received the M.Sc.E.E. degree from Aalborg University, Denmark, in 1983 with specialization in biomedical engineering. In 1988, he finished his Ph.D. dissertation made as a joint-venture project between University of Calgary, Calgary, Alta., Canada, and Aalborg University. He received the Dr.Med. degree in January 1998.

From 1984 to 1986, he studied at the Department of Clinical Neurosciences, University of Calgary and from 1989 to 1990 at Department of Physiology, Northwestern University, Chicago, IL. Since 1986, he has been an employee at Department of Medical Informatics and Image Analysis as an Associate Professor, in 1992 as Head of the department, and recently as research council professor and head of Center for Sensory-Motor Interaction established in 1993. In 1997, he became Professor in "Motor Control and Rehabilitation" at Aalborg University. His research interests include the application of natural sensors in FES systems, electrophysiology, biomechanics and motor control (human sensory-motor interaction). He has written more than 100 scientific papers published in international journals.

Dr. Sinkjær holds several offices: as member of "The Board of the Danish Research Councils" appointed by the Danish Minister of Research, Expert for the EC (DG XIII) Programme *Biomed II and Telematic (TIDE, DG XII)* and as referee for international journals, such as the *Journal of Neurophysiology* and the IEEE TRANSACTION ON REHABILITATION ENGINEERING. He is a member of IFESS (member of board of directors), The International Society of Postural and Gait Research, International Federation for Medical and Biological Engineering and Society of Neuroscience. He was rewarded with the prestigous Villum Kann Rasmussen's Yearly Grant for Outstanding International Research in 1996.